Supporting Information

Resende et al. 10.1073/pnas.1000979107

SI Materials and Methods

Eggs and Embryos. Fertilized *Gallus gallus* eggs were incubated at 37 °C in a 49% humidified atmosphere and staged according to Hamburger and Hamilton (HH) (1). A somite was considered to be completely formed when a definite cleft separating it from the PSM was observed (2).

RNA Probes. Antisense digoxigenin-labeled RNA probes were produced as previously described: *shh* (3), *hairy2* (4), *lunatic fringe* (5), *fgf8* (6), *raldh2* (7), *patched-1* (8), *patched-2* (9), *gli1* and *gli2* (10), *gli3* (11), *axin2* (12), *pax3* (13), *sprouty1* (14), and *meis2* (15). S*moothened* probe was generated by amplifying a 1,200-bp fragment of chick *smoothened* (XM_414970) using the sense 5′-TACTCACCGTGGCCATCCTG-3′ and antisense 5′-TCCTTC-TTCTTCTTCCTCCGCT-3′ oligos. The construct was confirmed by sequencing.

Explant Cultures. Chick embryos in stages HH10–14 were used. Ventrally positioned embryos were divided into two halves by cutting across the three germ layers at the midline level, either parallel to the embryonic axis or bisecting the axial structures (see below). For all explants, a second cut was made above the second formed somite and a third one immediately above the Hensen's node (HN) to prevent the addition of new cells to the PSM over time. Tissues thus delimited and excised created control and experimental explants, which were cultured individually, in a dorsal position, as previously described (16). Similar results were obtained in all experimental conditions tested whether the control/experimental explants were the left or right one. Number of somites formed was assessed after clearing the explants in formamide.

Notochord ablation. A cut was made parallel to the embryonic axis and along the neural tube so that only one explant possessed the notochord and the floor plate of the neural tube. For graft experiments, clumps of either QT6 quail fibroblasts stably transfected with an empty vector (QT6-ctrl) or with a construct carrying the SHH-coding region (QT6-Shh) (17) were juxtaposed to the No^- experimental explants.

In the retinoic acid (RA) treatment experiments, explants without notochord were cultured for 9 h in medium containing 15 μM of RA (Sigma), whereas the controls were incubated with DMSO (18). For FGF pathway induction studies, experimental explants (No^-) were incubated in medium containing mouse FGF8 (R&D Systems) at 250 ng/mL (19), whereas controls were incubated in PBS^--containing medium. To inhibit the FGF pathway, explants with notochord (No^+) were incubated in medium with 50 μM of SU5402 (Calbiochem), whereas controls were incubated in the presence of DMSO.

Notochord splitting. A longitudinal cut was performed bisecting both neural tube and notochord, producing two equivalent No^+ explants. For Shh chemical inhibition, experimental explants were cultured for 9 h in medium with 10 μg/mL cyclopamine (Calbiochem) or 25 μg/mL forskolin (Sigma), whereas the controls were incubated in DMSO-supplemented medium.

In the RA overexpression experiments, explants without notochord were cultured for 9 h in medium containing increasing RA (Sigma) concentrations (15, 30, and 100 μM), whereas the controls were incubated in DMSO-supplemented medium.

For the Shh overexpression studies, clumps of either QT6-ctrl or QT6-Shh cells (17) were juxtaposed to the No^+ experimental explants. In the combined SHH/RA treatments, clumps of QT6-Shh cells were juxtaposed to No^+ explants and were incubated in medium supplemented with 15 μM of RA.

In Ovo Microsurgery. Microsurgery was performed in ovo in embryos staged HH8–9. Indian ink was injected under the embryo to improve contrast, and a longitudinal surgical slit lateral to the notochord was performed, from the last formed somite to HN. Operated embryos were reincubated, after which they were treated for in situ hybridization.

In Situ Hybridization. In situ hybridization was performed as previously described (20). Background staining was reduced by using 1× SSC hybridization solution. Explant pairs were processed simultaneously, stained for the same amount of time and photographed using an Olympus SZX16 stereomicroscope.

In Situ Hybridization on Paraffin Sections. Stage HH13 or HH9 embryos were collected and fixed overnight in a solution containing 60% ethanol, 30% formaldehyde, and 10% acetic acid. Embryos were dehydrated in a series of ethanol dilutions of ethanol and washed in xylene. Finally, they were embedded in paraffin in the desired orientation. Transversal sections of 10 μm were made using Microm HM325 on SuperFrost Plus (Menzel-Glaser) slides and allowed to dry at 37 °C overnight. In situ hybridization on paraffin sections was performed as described previously (21).

Cross-Section Preparation. Hybridized embryos were embedded in Technovit 7100 (Heraus Kulzer GmbH) and sectioned using the automatic microtome Leica RM2155. Mounted sections were photographed using Olympus B BX61 microscope.

TUNEL Assay. Apoptosis was analyzed using the Cell Death Detection Kit (Roche) in explants with or without notochord, incubated for 9 or 12 h. Explants were fixed overnight in 4% paraformaldehyde (PFA) in PBS, permeabilized with PBS/0.5% Triton X-100/0.1% sodium citrate for 20 min at room temperature, and washed in PBS. Positive control embryos were incubated with DNase at 37 °C for 1 h. Embryos and explants were incubated overnight at 37 °C with the TUNEL solution mix and washed at least three times in PBS before visualization.

PH3 Immunohistochemistry (IHC). Whole-mount IHC for PH3 was performed in explants with or without notochord, incubated for 9 or 12 h to analyze cell proliferation. Explants were fixed in 4% PFA in PBS and permeabilized with 0.5% Triton X-100 in PBS for 3 h. Explants were incubated in blocking solution (PBS 1% Triton/10% FBS/0.2% sodium azide) twice for 1 h. Endogenous peroxidases were block by incubating explants in blocking solution containing 0.1% H2O2. Primary antibody incubation with rabbit anti-phospho-histone H3 (UBI) (1/100, diluted in blocking solution) was performed overnight at 4 °C, followed by washes in blocking solution. Explants were washed in PBS 1% Triton to remove all azide, followed by secundary antibody incubation overnight at 4 °C (biotinylated goat anti-polyvalent, Ultravision detection system; Lab Vision). After PBS 1% Triton washes, explants were incubated in DAB substrate (Ultravision detection system; Lab Vision) for 2 h. Fresh DAB plus H_2O_2 was then added. Explants were incubated until staining reached the desired intensity and were washed with PBS.

Time-Lapse Imaging. For time-lapse experiments, embryos at stages HH3–5 were removed from the egg, placed in New culture (22), and reincubated until six to eight somites stage (HH8–9). In each embryo, a small incision was made lateral to the notochord across the three germ layers and along the length of four to seven pre-

sumptive somites. Embryo cultures were maintained at 37.5 °C and 90% humidity and observed using a Leica DMIRE2 inverted microscope equipped with a Hamamatsu EM-CCD digital camera. Images were acquired with a 2.5× NA 0.07 objective using Image-Pro Plus software (Media Cybernetics). Photographs were collected every 5 min during a period of 10 h of incubation. Image series were recorded as TIFF files and processed using ImageJ software (http://rsb.info.nih.gov/ij/) to correct embryo drift and to adjust contrast and brightness.

Statistical Analysis. Quantitative data are presented as mean value ± SD and were analyzed using the SigmaStat3.5 software (Systat Software, Inc.). Statistical significance was set at $P < 0.01$ or $P < 0.05$, as indicated.

1. Hamburger V, Hamilton HL (1992) A series of normal stages in the development of the chick embryo. 1951. *Dev Dyn* 195:231–272.
2. Pourquie O, Tam PPL (2001) A nomenclature for prospective somites and phases of cyclic gene expression in the presomitic mesoderm. *Dev Cell* 1:619–620.
3. Riddle RD, Johnson RL, Laufer E, Tabin C (1993) Sonic hedgehog mediates the polarizing activity of the ZPA. *Cell* 75:1401–1416.
4. Jouve C, et al. (2000) Notch signalling is required for cyclic expression of the hairy-like gene HES1 in the presomitic mesoderm. *Development* 127:1421–1429.
5. Sakamoto K, et al. (1997) Identification of a chick homologue of Fringe and C-Fringe 1: Involvement in the neurogenesis and the somitogenesis. *Biochem Biophys Res Commun* 234:754–759.
6. Crossley PH, Minowada G, MacArthur CA, Martin GR (1996) Roles for FGF8 in the induction, initiation, and maintenance of chick limb development. *Cell* 84:127–136.
7. Tsukui T, et al. (1999) Multiple left-right asymmetry defects in Shh2/2 mutant mice unveil a convergence of the Shh and retinoic acid pathways in the control of Lefty-1. *Proc Natl Acad Sci USA* 96:11376–11381.
8. Marigo V, Tabin CJ (1996) Regulation of Patched by Sonic hedgehog in the developing neural tube. *Proc Natl Acad Sci USA* 93:9346–9351.
9. Pearse RV, Vogan KJ, Tabin CJ (2001) Ptc1 and Ptc2 transcripts provide distinct readouts of hedgehog signaling activity during chick embryogenesis. *Dev Biol* 239:15–29.
10. Marigo V, Scott MP, Johnson RL, Goodrich LV, Tabin CJ (1996) Conservation in hedgehog signaling: Induction of a chicken patched homolog by Sonic hedgehog in the developing limb. *Development* 122:1225–1233.
11. Borycki A-G, Brown AMC, Emerson JCP (2000) Shh and Wnt signaling pathways converge to control Gli gene activation in avian somite. *Development* 127:2075–2087.
12. Gibb S, et al. (2009) Interfering with Wnt signalling alters the periodicity of the segmentation clock. *Dev Biol* 330:21–31.
13. Goulding MD, Lumsden A, Gruss P (1993) Signals from the notochord and floor plate regulate the region-specific expression of two Pax genes in the developing spinal cord. *Development* 117:1001–1016.
14. Eloy-Trinquet S, Wang H, Edom-Vovard F, Duprez D (2009) Fgf signaling components are associated with muscles and tendons during limb development. *Dev Dyn* 238: 1195–1206.
15. Heine P, Dohle E, Bumsted-O'Brien K, Engelkamp D, Schulte D (2008) Evidence for an evolutionary conserved role of homothorax/Meis1/2 during vertebrate retina development. *Development* 135:805–811.
16. Palmeirim I, Henrique D, Ish-Horowicz D, Pourquie O (1997) Avian hairy gene expression identifies a molecular clock linked to vertebrate segmentation and somitogenesis. *Cell* 91:639–648.
17. Duprez D, Fournier-Thibault C, Le Douarin N (1998) Sonic Hedgehog induces proliferation of committed skeletal muscle cells in the chick limb. *Development* 125: 495–505.
18. Diez del Corral R, et al. (2003) Opposing FGF and retinoid pathways control ventral neural pattern, neuronal differentiation, and segmentation during body axis extension. *Neuron* 40:65–79.
19. Olivera-Martinez I, Storey KG (2007) Wnt signals provide a timing mechanism for the FGF-retinoid differentiation switch during vertebrate body axis extension. *Development* 134:2125–2135.
20. Henrique D, et al. (1995) Expression of a Delta homologue in prospective neurons in the chick. *Nature* 375:787–790.
21. Tozer S, et al. (2007) Involvement of vessels and PDGFB in muscle splitting during chick limb development. *Development* 134:2579–2591.
22. New DAT (1955) A new technique for the cultivation of the chick embryo in vitro. *J. Embryol Exp Morph* 3:326.

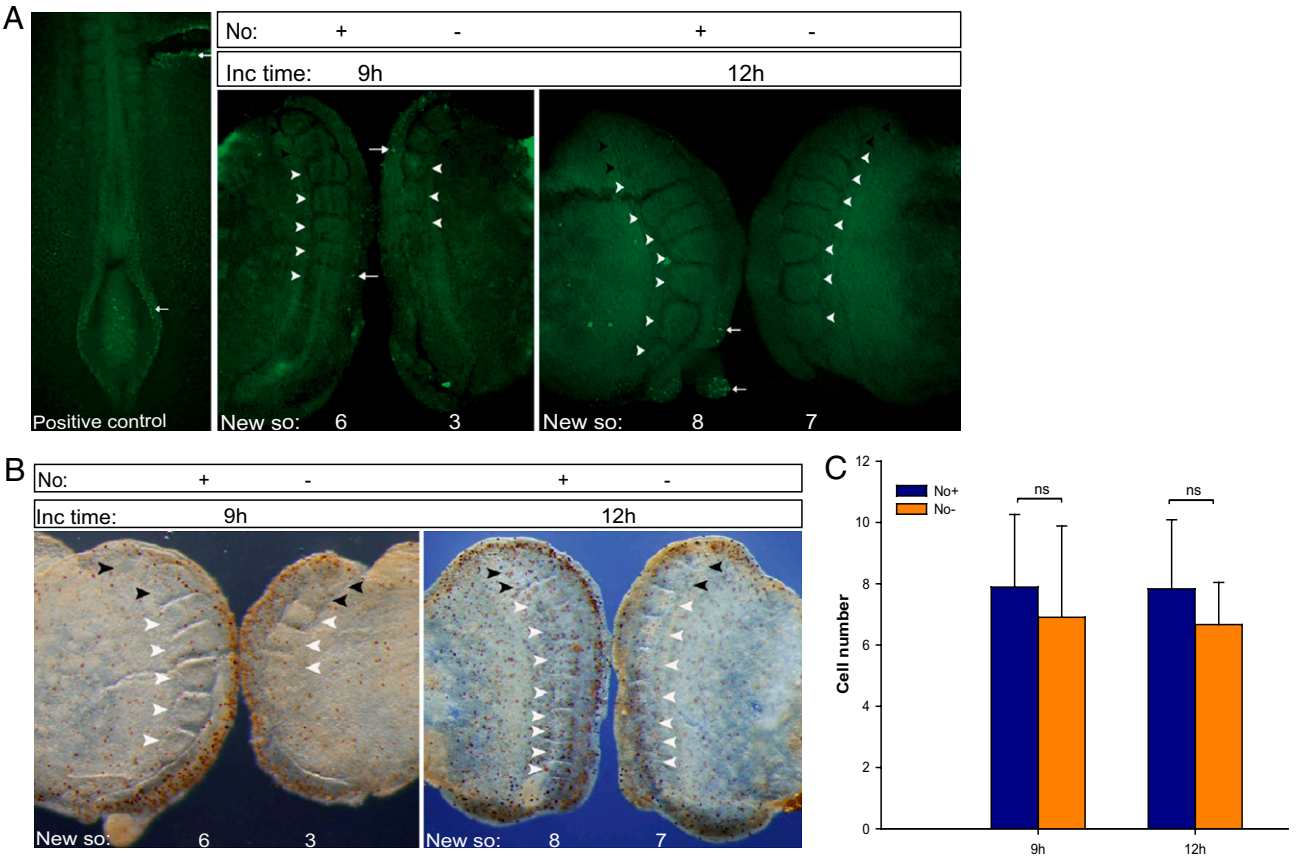

Fig. S1. Alterations in levels of cell death or proliferation cannot account for somite formation delay in notochord-ablated PSMs. (*A*) PSM cell apoptosis was assessed by performing TUNEL assay in explants with (No^+) or without (No^-) notochord incubated separately for 9 h or 12 h. A positive control for the assay is shown. White arrows point to specific TUNEL staining. (*B*) Explants with (No^+) or without (No^-) notochord and incubated for 9 h or 12 h were processed for immunohistochemistry with PH3 antibody. Number of somites formed during culture (New so) is indicated. Black arrowheads indicate somites formed before culture; white arrowheads point to somites formed during the incubation period. (*C*) Graphic representation of PH3 staining in explants with (No^+) or without (No^-) notochord ($n = 3$). Data are mean ± SD. ns, not statistically significant.

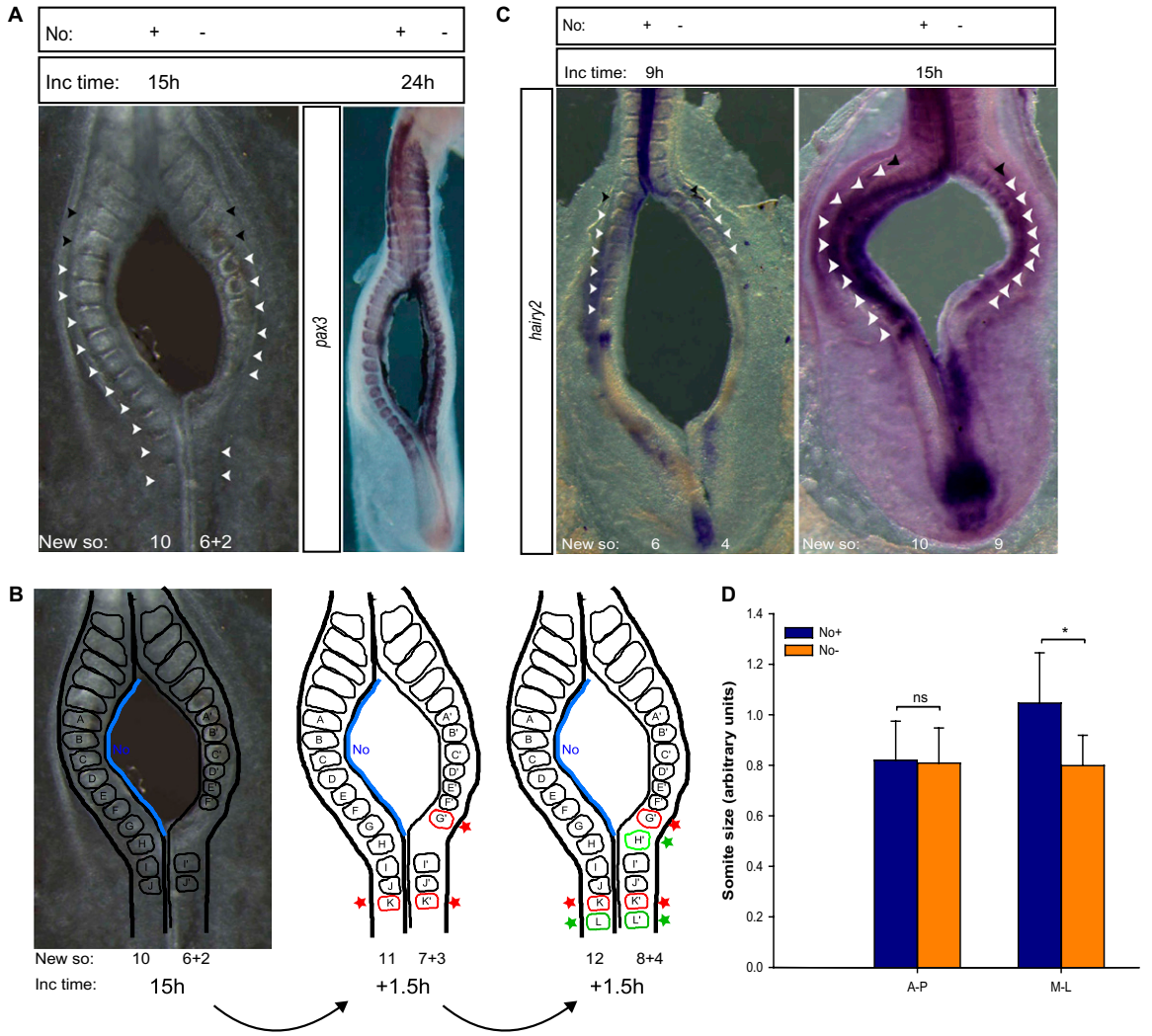

Fig. S2. Notochord ablation in ovo delays, but does not halt, somite segmentation of undetermined PSM. (*A*) Representative results obtained in in ovo operated embryos after a reincubation period of 15 h and 24 h, showing incomplete and complete segmentation of notochord-ablated tissue, respectively. Embryos incubated for 24 h were processed for *pax3* in situ hybridization for somite visualization. (*B*) Representation of how somite number is recovered in No^- PSM tissue. Figure of 15-h incubated embryo has been outlined, and somites formed upon incubation are marked alphabetically. During the incubation period, timely somite formation proceeded in the No^+ PSM, reaching the tissue caudal to the slit, where timely bilateral somite formation was resumed. Meanwhile, there is a delay in somite segmentation in the notochord-deprived PSM, resulting in a gap of unsegmented tissue of approximately a 2-somite length at the posterior end of the slit. When somite formation rate is recovered in No^- PSM, timely somite formation proceeds in the unsegmented gap, so that during the next 1.5 h a new pair of somites will be formed in the PSM (somites K-K′, red), concomitantly with an extra somite in the No- tissue facing the surgical slit (somite G′, red). The same is true for the next 1.5 h: Somite pair L-L′ is formed, as well as somite H′ (green). (*C*) In ovo operated embryos in situ hybridized for *hairy2* after reincubation periods of 9 h and 15 h, showing concomitant deregulation of molecular clock with somite formation delay. Presence (No^+) or absence (No^-) of notochord, and number of somites formed during reincubation (New so), are indicated. Black arrowheads indicate somites formed before culture; white arrowheads indicate somites formed during the incubation period. (*D*) Graphic representation of mean size of somites formed in the presence (No^+) or absence (No^-) of the notochord, along both anterior–posterior (A-P) and medial–lateral (M-L) axes. Data are mean ± SD. $*P < 0.01$. ns, not statistically significant.

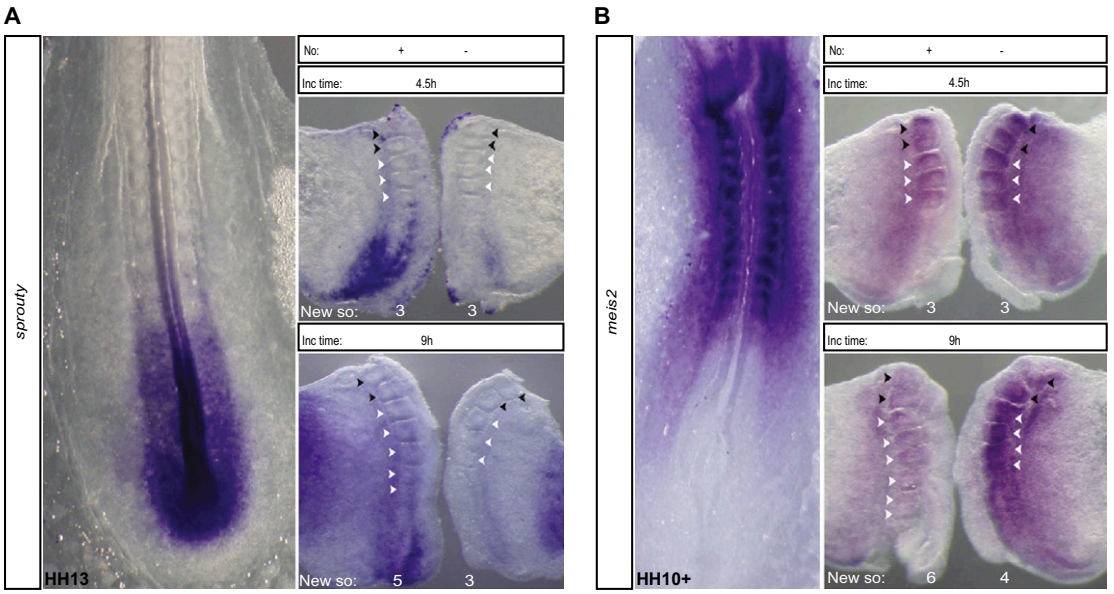

Fig. S3. Notochord ablation alters FGF and RA signaling readouts. (*A* and *B*) Expression patterns of *sprouty* and *meis2*, downstream targets of FGF and RA, respectively, evaluated by in situ hybridization in explants cultured for 4.5 or 9 h. Presence (No^+) or absence (No^-) of notochord is indicated. Black arrowheads indicate somites formed before culture; white arrowheads indicate somites formed during incubation (New so).

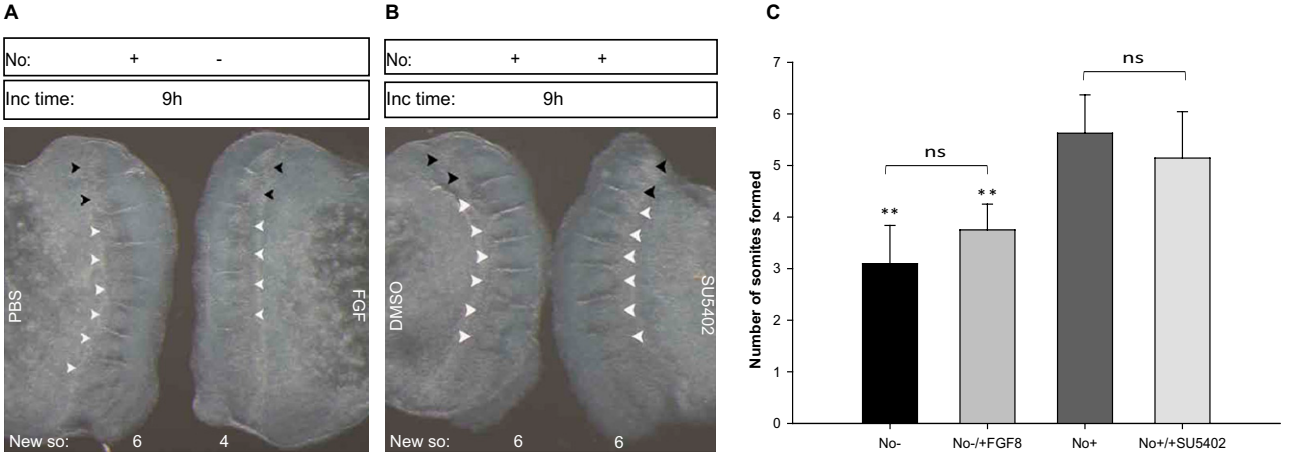

Fig. S4. Somite formation delay in absence of notochord is primarily due to an impairment of FGF signaling. (*A*) Explants with (No^+) or without (No^-) notochord were cultured for 9 h with PBS (control explant) or with 250 ng/mL FGF8 (experimental explant). (*B*) Explants with (No^+) notochord were cultured for 9 h with DMSO (control explant) or with 50 μM SU5401 (experimental explant). Black arrowheads indicate somites formed before culture; white arrowheads indicate somites formed during incubation period (New so). (*C*) Graphic representation of mean values of the number of somites formed by explants without notochord (No^-), without notochord incubated with FGF8 (No^-/+FGF), with notochord (No^+), or with notochord and SU5402 (No^+/+SU5402). $^{**}P < 0.05$ vs. No^+ or No^+/+SU5402. ns, not statistically significant. Data are mean ± SD.

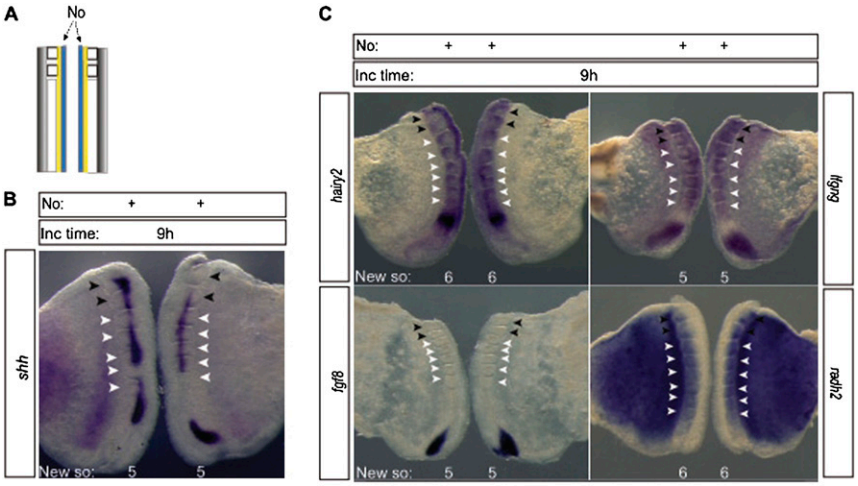

Fig. S5. Presence of notochord ensures timely somite formation and molecular segmentation. (*A*) Symmetrical explants, both containing notochord tissue, were generated by surgically cutting both the neural tube and notochord down the midline. (*B*) Because of the harshness of the notochord, it was not always possible to perfectly bisect it, as denoted by hybridization with notochord marker *shh*. (*C*) Although sometimes discontinuous, the presence of notochord tissue ensures normal somite segmentation rate, as 98% of the explants pairs present the same number of somites after a 9-h incubation ($n = 34$), in contrast to only 5% when the notochord is confined to half ($n = 90$). Whole-mount in situ hybridization of these explants clearly shows that the molecular clock genes *hairy2* and *lfng* present similar expression patterns in symmetrical explants, and no alterations are observed for *fgf8* and *raldh2*. Presence of notochord (No^+) and number of somites formed (New so) are indicated. Black arrowheads indicate somites formed before culture; white arrowheads point to somites formed during the incubation period.

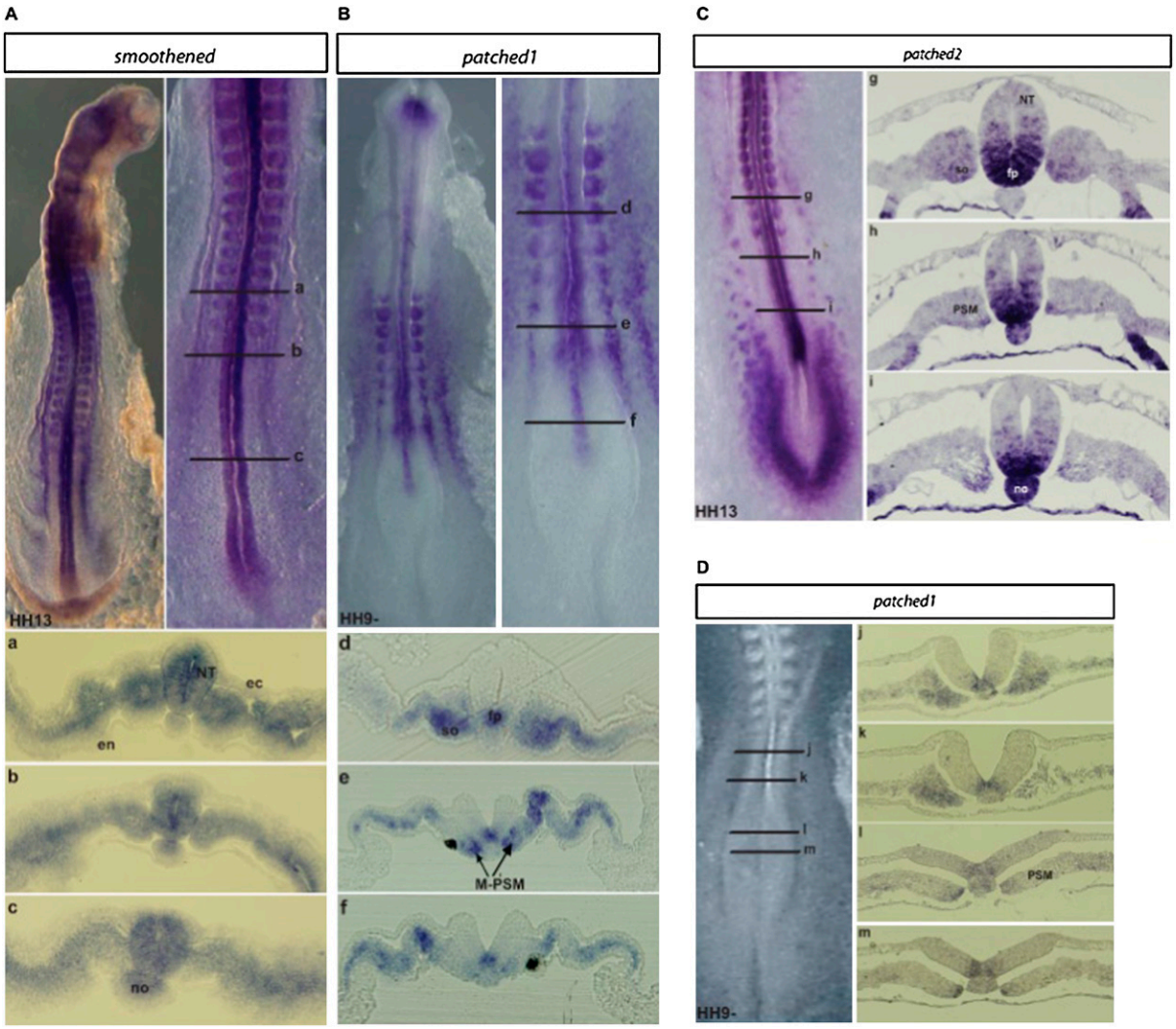

Fig. S6. Expression patterns of Shh signaling components *smoothened*, *patched1,* and *patched2*. Chicken embryos from HH9-15 were processed for in situ hybridization using a probe for *smoothened, patched1,* or *patched2,* and representative results are shown. (*A*) *Smo* is expressed in neural tube (NT) and throughout all mesoderm-derived tissues, including PSM and notochord (no), but is absent in ectoderm (ec) and endoderm (en). In epithelialized tissues, *smo* is preferably localized in the cells' apical region (Aa). (*B*) *Ptch1* is expressed in the ventral part of somites (so) and neural tube floor plate (fp). Upon increased staining, *ptch1* was also visible in the most medial PSM (M-PSM), just adjacent to notochord (Be). (*C*) In situ hybridization in paraffin sections shows that *ptch2* is expressed in the ventral part of somites (so), neural tube floor plate (fp), notochord (no), and also in the most medial portion of the PSM. (*D*) In situ hybridization in paraffin sections suggests an anterior–posterior gradient of *ptch1* expression in M-PSM region. Black lines indicate anterior–posterior levels of transverse sections.

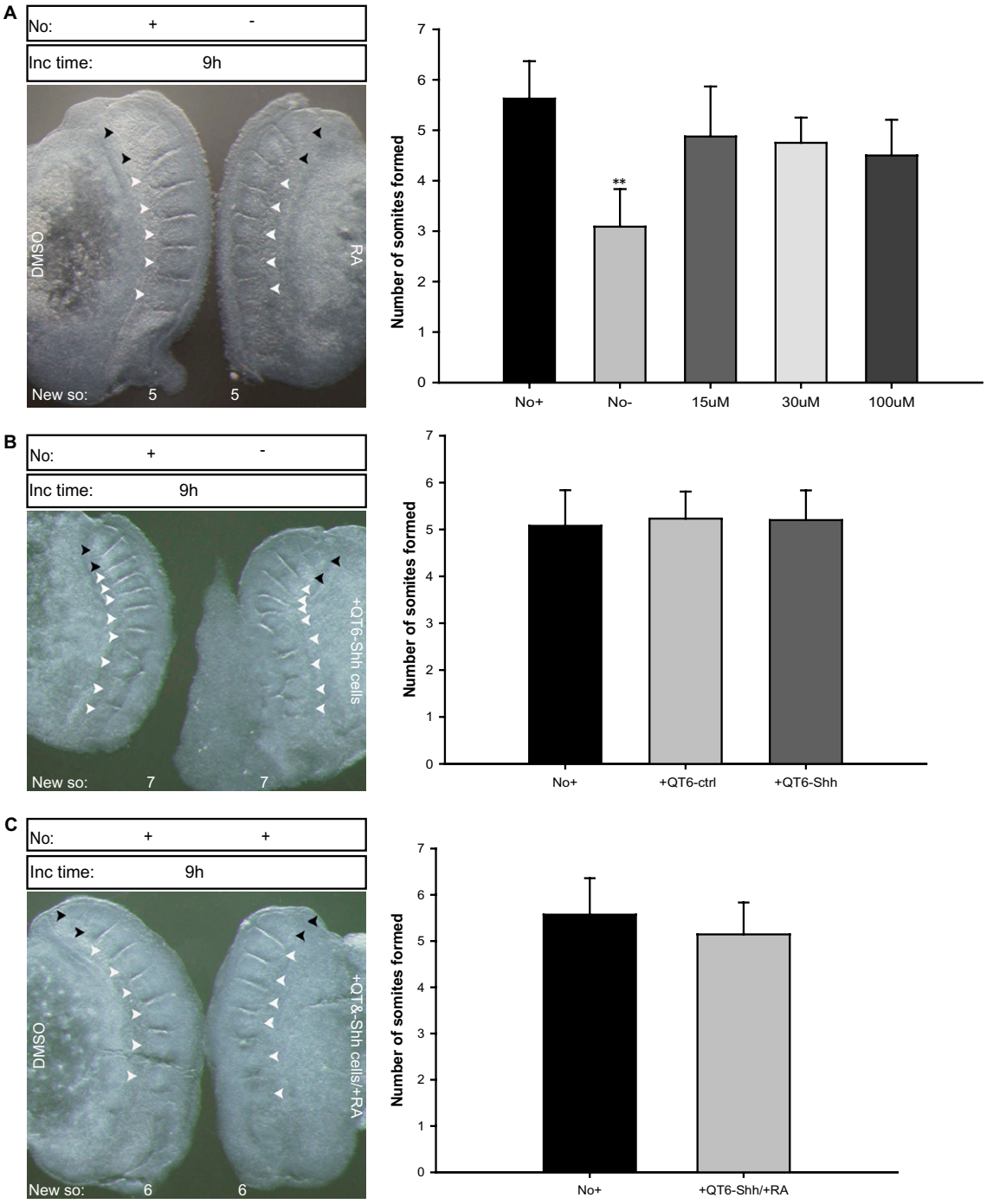

Fig. S7. Overexpression of RA, Shh or both does not lead to a faster PSM segmentation rate. (*A*) Explants with (No^+) or without (No^-) notochord were cultured for 9 h with DMSO (control explant) or with increasing concentrations of retinoic acid (RA) (experimental explant). Graphic representation of mean number of somites formed by explants with notochord (No^+), without notochord (No^-), or without notochord but with increasing concentrations of RA (μM). $^{**}P < 0.05$ vs. No^+ or different RA concentrations. (*B*) Explants with (No^+) notochord alone (control explant) or juxtaposed to a clump of QT6-producing Shh cells (QT6-Shh, experimental explant) were cultured for 9 h. Graphic representation of mean number of somites formed by explants with notochord (No^+) and with notochord and juxtaposed control (+QT6-ctrl) or Shh-producing (+QT6-Shh) cells. (*C*) Explants with (No^+) notochord (control explant) or with a clump of QT6-producing Shh cells and 15 μM of RA (+QT6-Shh/+RA, experimental explant) were cultured for 9 h. Graphical representation of mean values of number of somites formed by explants with notochord (No^+) or with notochord plus QT6-Shh cells and RA (+QT6-Shh/+RA). Data are represented as mean ± SD. Black arrowheads indicate somites formed before culture; white arrowheads indicate somites formed during incubation period (New so).

Fig. S8. Somite formation delay in absence of Shh is not due to impairment of Wnt signaling pathway. Representative results of *axin2* expression in HH13 whole embryo and in No^+/No- explants incubated for 4.5 h and 9 h. Presence (No^+) or absence (No^-) of notochord and number of somites formed during reincubation (New so) are indicated. Black arrowheads indicate somites formed before culture; white arrowheads point to somites formed during incubation period. Expression of *axin2* is unaltered in 60% of notochord-ablated explants, and expression in the other 40% is only slightly down-regulated after 4.5 h. After 9 h, *axin2* is clearly down-regulated in all explants tested. *Axin2* down-regulation after 9 h of incubation is a predictable result from our proposed model (Fig. 7), according to which Gli2/3 repressor forms are abundant in PSM up to this time due to the absence of Shh signaling; Gli3R has been shown to inhibit *axin2* expression (1), so *axin2* down-regulation seems likely to be a consequence of Shh deprivation. Some reports position Shh pathway upstream of Wnt (2, 3) and our results suggest that this could be the case in the PSM, although we do not wish to argue such at this time. It is also very unlikely that a reestablishment of Wnt signaling is the primary event leading to the recovery of timely PSM segmentation after 9 h of Shh deprivation, as *axin2* is down-regulated at this time point. Overall, the results strongly suggest that Wnt signaling is not the primary cause of the segmentation delay observed in the absence of Shh.

1. Ulloa F, Itasaki N, Briscoe J (2007) Inhibitory Gli3 activity negatively regulates Wnt/beta-catenin signaling. *Curr Biol* 17:545–550.
2. Alvarez-Medina R, Le Dreau G, Ros M, Martí E (2009) Hedgehog activation is required upstream of Wnt signalling to control neural progenitor proliferation. *Development* 136: 3301–3309.
3. Miyagawa S, et al. (2009) Dosage-dependent hedgehog signals integrated with Wnt/beta-catenin signaling regulate external genitalia formation as an appendicular program. *Development* 136:3969–3978.

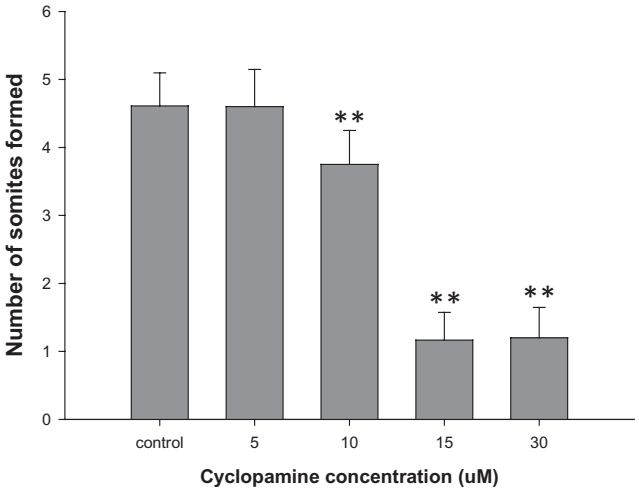

Fig. S9. Shh inhibition delays somite formation in a dose-dependent manner. Graphic representation of mean number of somites formed by explants with notochord (No^+), in the presence of either DMSO (control) or increasing concentrations of cyclopamine after a 9-h incubation. $^{**}P < 0.05$ vs. control. Data are represented as mean ± SD.

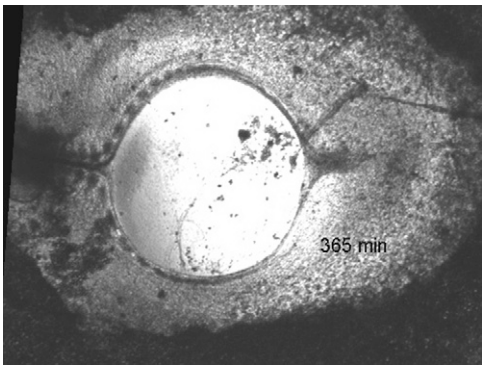

Movie S1. Real-time imaging of somite formation delay in notochord-deprived PSM. A small incision was made lateral to the notochord across the three germ layers and along the length of four to seven presumptive somites in six- to eight-somite–stage embryos grown in New culture (1). Embryo cultures were placed in a custom-built air-heated microscope chamber and maintained at 37.5 °C and 90% humidity. Somite formation was imaged over time, and a representative result is shown. In this case, the slit included anteriorly two previously formed somites. The segmentation of the three first somites formed after the microsurgical incision proceeded at the same rate in both PSMs (No^+, top; No^-, bottom). The formation of the subsequent somites was delayed in the PSM deprived of the notochord/floor plate, whereas the No^+ PSM segmented at the normal rate of one somite/90 min.

Movie S1